INDIAN JOURNAL OF SCIENCE AND TECHNOLOGY

RESEARCH ARTICLE

OPEN ACCESS

Received: 23-01-2024

Accepted: 12-02-2024

Published: 05-03-2024

Citation: Sathishkumar GB, Asaithambi B, Srinivasan V (2024) Optimizing Laser Cladding Parameters on AZ61 Magnesium Alloy with Inconel 625 Powder through Grey Relation Analysis. Indian Journal of Science and Technology 17(11): 1059-1069. https://doi.org/10.17485/IJST/v17i11.2686

* **Corresponding author**.

gbsathishkumarmech@gmail.com

Funding: None

Competing Interests: None

Published By Indian Society for Education and Environment (iSee)

ISSN
Print: 0974-6846
Electronic: 0974-5645

Optimizing Laser Cladding Parameters on AZ61 Magnesium Alloy with Inconel 625 Powder through Grey Relation Analysis

G B Sathishkumar[1]*, B Asaithambi[2], V Srinivasan[3]

1 Research Scholar, Department of Manufacturing Engineering, Faculty of Engineering and Technology, Annamalai University, Annamalai Nagar, Chidambaram, 608002, Tamil Nadu, India

2 Assistant Professor, Department of Manufacturing Engineering, Faculty of Engineering and Technology, Annamalai University, Annamalai Nagar, Chidambaram, 608002, Tamil Nadu, India

3 Associate Professor, Department of Manufacturing Engineering, Faculty of Engineering and Technology, Annamalai University, Annamalai Nagar, Chidambaram, 608002, Tamil Nadu, India

Abstract

Objective: To investigate the mechanical and tribological behaviors of the surface-modified AZ61 alloy reinforced with Inconel 625 using the laser cladding method. **Methodology:** Surface modification was done with the help of a laser cladding machine by changing the input parameters such as Laser Power (LP), Scanning Speed (SS) and Powder Feed Rate (PFR). Experimentation was done as per L9 Taguchi design, and Grey Relational Analysis (GRA) was used to optimize the input parameters of surface-modified AZ61 alloy reinforced with Inconel 625 particles for measuring the output responses microhardness and wear rate. **Findings:** Based on the experimental findings, it was observed that laser power accounts for 76.13% of the variation in microhardness, while the powder feed rate predominantly affects wear volume, influencing it by 61.9%, as confirmed by grey relational grade analysis. To identify the most suitable processing parameters across different objectives, this study employs the grey relational method. The outcomes indicate that the microhardness and wear volume of the composite are notably impacted by the Inconel 625 powder feed rate. By integrating Grey relational analysis with multiple optimization objectives, a transparent method is established, resulting in a clad material with higher microhardness and reduced wear volume. The optimized processing parameters forecasted grey relational grades with a negligible error rate of 1.89%, with a significant contribution of 75.17% attributed to laser power. This investigation underscores the potential of multi-objective optimization in improving the mechanical properties of laser-cladded surfaces and establishes a theoretical framework for this approach. **Novelty:** This research work exhibits a unique method to modify the surface of the substrate by reinforcing Inconel 625 particle as a dense coating by adopting laser cladding technique.

Keywords: Inconel 625; Laser Cladding; Optimization; GRA

1 Introduction

In recent years, industries have increasingly focused on enhancing the mechanical, corrosion and wear resistance properties of materials, particularly for applications in automotive, aerospace and marine sectors where durability demand is in challenging conditions. Magnesium alloys, being lighter yet stronger, have gained considerable attention and widespread use across various industries[1,2]. Mg alloys offer upto 70% weight reduction when compared to stainless steel and are 33% lighter than aluminum, alongside advantages like ease of handling, high damping capacity, and affordability. However, the wear behavior of magnesium alloys is less understood when compared to other materials[3]. Wear, generally defined as surface degradation through continuous friction, is particularly critical for magnesium alloys in vital automotive applications. Surface modification becomes crucial in contexts where wear and corrosion resistance are vital, especially given magnesium's inherent reactivity.

Several studies have focused on improving the functionality and longevity of magnesium alloys by surface reinforcement, aiming to enhance their mechanical, wear and corrosion characteristics. In automotive applications requiring high wear and corrosion resistance, Fe-based and Ni-based alloys are often chosen for laser cladding as base materials. The use of hard chrome coatings is increasingly being restricted due to the environmental and health hazards posed by hexavalent chromium (Cr6+), identified by the World Health Organization as carcinogenic[4]. This scenario necessitates a shift towards more environmental friendly alternatives to traditional hard chrome coatings. Conventionally, techniques such as cold spray[5], Electroless Nickel Plating (ENP)[6], and Plasma Electrolytic Oxidation (PEO)[7] have been used to apply hard chrome coatings on automotive components for wear and corrosion resistance. However, laser cladding has emerged as a more advanced surface modification technology, offering superior physical and chemical properties. This technique enables the production of dense, crack-free, high-quality multi-layered coatings, marking a significant improvement over conventional plating technology[8]. Laser cladding is renowned for its capability to deposit Inconel 625 alloy coatings that are free of cracks and exhibit low porosity. Yet, the complexity of its control parameters presents challenges in consistently achieving high-quality coatings.

Shayanfar et al.[9] used regression to evaluate Inconel 625 powder deposition on an ASTM A592 steel substrate and clad height, width, and depth and LC dilution rate. Geometric features correlated linearly with processing parameters. They created a processing parameter process map for good clad quality. Fan et al.[10] focuses on optimizing the process for WC-Co50 cermet composite coating by laser cladding. Taguchi orthogonal experimental design was used to investigate the correlation between processing parameters and cladding quality. The results show that the WC powder ratio and laser power have a significant impact on micro-hardness, wear resistance and cladding efficiency. Grey relational analysis was used to optimize the processing parameters and achieve the desired combination of multiple objectives. The study provides valuable insights into improving the quality of the WC-Co50 cermet composite coating deposited by laser cladding. Yi et al.[11] explored the impact of laser parameters on graphite morphology in the bonding zone and optimized the process in gray cast iron laser cladding. The study investigated how laser settings influenced the appearance of graphite in the bonding zone. By analyzing the graphite morphology, the authors aimed to understand the relationship between laser parameters and the quality of the cladding process. The findings contribute to optimizing laser cladding processes for gray cast iron, providing insights which can enhance the overall performance and quality of the resulting structures. Wu et al.[12] investigated the use of laser cladding for repairing or restoring the used parts to their original condition. Experiments were conducted to optimize the process parameters for Ni60A alloy coating using response surface methodology. This work insights into the optimal processing parameters for laser cladding in remanufacturing applications and offers a useful approach for determining the best coating properties and a potential solution for remanufacturing applications.

Sundaraselvan et al. studied the use of laser cladding to modify the surface of magnesium alloy with nano-Al_2O_3 to improve its wear resistance. The authors conducted experiments with different processing parameters and used the GRA-PCA method to optimize the wear properties[13]. Several researchers focused on Mg alloys reinforcing particles of TiO_2/Al_2O_3 [13], Ni60[14], Al-TiC-Y_2O_3 [15], Al-SiC[16]. Extensive literature reviews indicate that laser cladding is an effective method for surface modification, leading to enhanced mechanical properties wear and corrosion properties. However, research on applying Inconel 625 powder to magnesium alloys via laser cladding remains limited[17–20]. Further, no reports were published on optimizing hardness and wear loss of AZ61 magnesium alloy laser cladded with Inconel 625. Thus, this study aims at to investigate the impact of various processing parameters, including LP, SS and PFR on the surface modification of magnesium alloy substrates.

2 Methodology

In this study, a commercially available AZ61 Mg alloy is chosen as the substrate material, with each specimen possessing specifications of 200 mm x 150 mm x 15 mm sourced as plates from Vision Castings and Alloys (Hyderabad). The elemental composition of the substrate is detailed in Table 1**(a)**. Micro structural examination of the AZ61 magnesium alloy was analyzed using Scanning Electron Microscopy (SEM) coupled with Energy Dispersive X-ray Analysis (EDAX), as depicted in Figure 1**(a & b)**. These images predominantly reveal the presence of magnesium particles, with EDAX quantification confirming magnesium as the principal element. Additionally, secondary constituents, aluminum, and zinc, were also detected through the EDAX analysis. Inconel 625 as the reinforcing agent for this research was sourced from Zhangzhou XiangchengYuteng Ceramic Products Co., Ltd (China) and had a particle size range of 40 to 120 microns, serving as the feedstock powder for reinforcing the substrate. Table 1 (**b**) provides the elemental composition of the Inconel 625 powder, while Figure 1 **(c & d)** displays its morphology, confirming the particle shape and size.

Table 1. Elemental composition

(a) Elemental composition (wt %) of AZ61 Magnesium Alloy

Material	**Element (wt %)**							
	Mg	Al	Zn	Mn	Si	Cu	Ni	Fe
AZ61	93.0	5.80 – 7.20	0.40 – 1.50	0.15	0.10	0.05	0.005	0.005

(b) Elemental composition (wt %) of Inconel 625 Powder

Powder	**Element (wt %)**						
	Ni	Cr	Mo	Nb	Al	Fe	Co
Inconel625	56.6	22.0	11.8	5.0	2.0	1.6	1.0

The Laser cladding equipment shown in Figure 2 was equipped with significant control parameters such as laser generation, powder feeding system, deposition system, and a PLC computer system. Prior to conducting laser cladding, thorough substrate surface preparation was carried out through cleaning with acetone, rinsing with alcohol, and thorough drying. LC is a complex process influenced by various factors. This study investigates the influence of three key factors: LP, SS and PFR, each at three different levels. Combinations of these factors through adopting a three-factor and three-level orthogonal array design, as presented in Table 2. This design allowed us to achieve optimal results with fewer experimental runs. Consequently, the L9 (3^3) Taguchi orthogonal array comprises a total of 9 trials, as detailed in Table 2. After completing the LC processes, obtained 9 surface modified samples were subjected to analyze microhardness and wear volume of the clad properties.

Microhardness test was conducted by examining the cross-section of the specimens using a Vickers hardness tester as per the ASTM E92 Standard. The microhardness of the laser-cladded AZ61 substrate was examined under a load of 300 grams and a dwell time of 12 seconds. During the microhardness testing, hardness values were measured at intervals of 0.1 mm from the surface to the interior of the processed AZ61 Mg alloy substrate, and the average value was calculated, as displayed in Figure 3**(a)**. The experimental setup of the Microhardness testing machine is shown in Figure 3 **(b)**[21].

Wear characteristics were measured and analyzed using a pin-on-disc apparatus, as illustrated in Figure 4. The dry sliding wear properties of the cladded specimens were investigated in accordance with ASTM G99 standards. Prior to the wear behavior test, specimens were cut by using Wire Electrical Discharge Machining (WEDM) to dimensions of diameter 10 mm and height

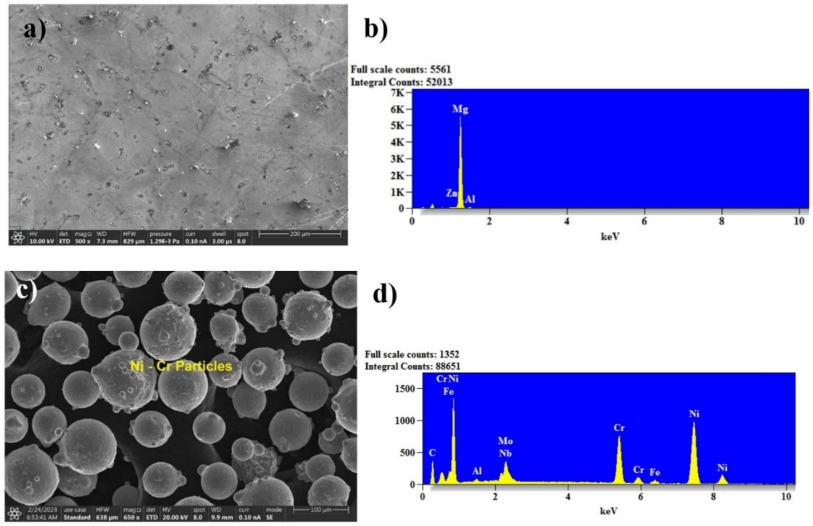

Fig 1. (a) SEM image of AZ61 magnesium alloy, (b) EDAX of AZ61 magnesium alloy as received condition, (c) SEM image of Inconel 625 powder, (d) EDAX of Inconel 625 powder

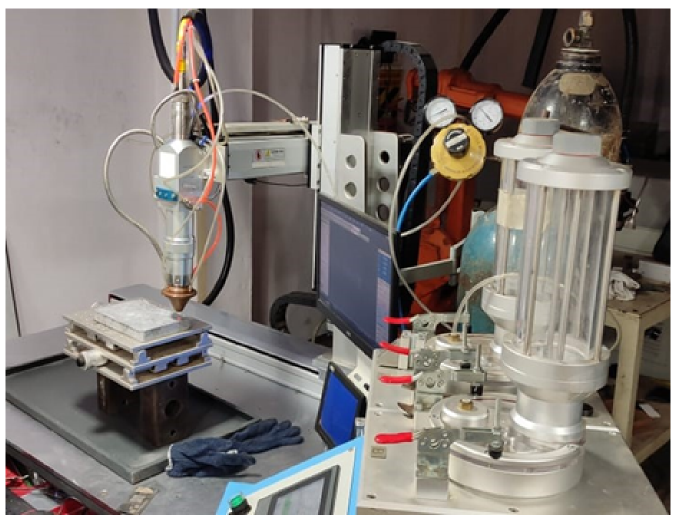

Fig 2. Experimental setup of Laser Cladding Machine

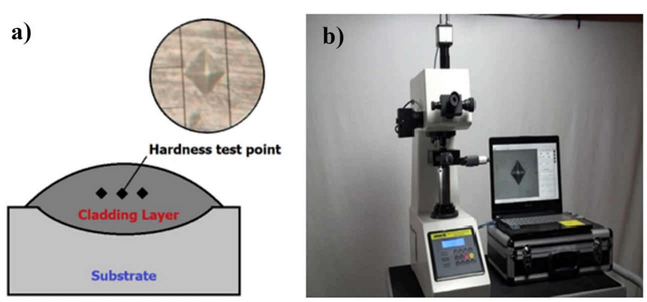

Fig 3. (a) Test Location of the Vickers indentation, (b) Vickers Microhardness Tester

30 mm from the modified surface specimens. The specimens were tested against a counter surface of EN 32 steel disc with a hardness of 60 HRC. Both surfaces were cleaned with acetone solvent before conducting the wear test. To examine the wear behavior of laser-cladded samples, an applied load of 20 N, sliding speed of 1.25 m/s, and sliding distance of 800 m were employed. The surface morphologies of the wear-tested cladded specimens were examined by using SEM to identify wear scars and mechanisms [22].

Fig 4. Pin on disc apparatus

3 Results and discussion

Laser cladding with Inconel 625 was used to modify AZ61 in accordance with the Taguchi experimental plan to design the plan, including variables such as laser power, scanning speed and powder feed rate. Microhardness and wear were examined in surface-modified AZ61 magnesium alloy. During this experiment, the hardness and wear conditions were recorded at room temperature. Table 2 shows that Taguchi's DoE was used to design an experiment to modify the surface with the selected variables as inputs and their levels.

Table 2. Expanded L9 of process parameters and output responses

Trial No	Laser power (kW)	Scanning speed (mm/s)	Powder feed rate (g/m)	Microhardness (HV)	Wear Volume (mm^3)
1	1.5	9	20	387.23	1.4091
2	1.5	10	25	412.13	1.3739
3	1.5	11	30	401.56	1.4702
4	1.6	9	25	441.17	1.3515
5	1.6	10	30	456.41	1.3912
6	1.6	11	20	454.82	1.4094
7	1.7	9	30	385.58	1.4255
8	1.7	10	20	427.35	1.3873
9	1.7	11	25	414.47	1.3706

The study employed the signal-to-noise (S/N) ratio technique, integrated with Taguchi analysis, to identify the optimal processing parameters for the laser cladding process. This S/N conversion is a crucial tool for optimizing data analysis and enhancing mechanical and tribological properties to achieve optimal values. Key responses such as microhardness and wear volume of the laser-cladded surface were of prime importance, with the criteria for selection being 'larger is better' for microhardness and 'lesser is better' for wear volume. The S/N ratio for these characteristics was calculated by using actual data extracted from Table 2. The outcomes of the S/N conversion, along with measured values for microhardness and wear volume are displayed in Table 3. Subsequently, Analysis of Variance (ANOVA) was employed to examine the factors influencing microhardness and wear volume by using a 95% confidence interval supported by Design of Experiments (DOE).

Table 3. Results of S/N conversion for microhardness and wear volume

Trial No.	Microhardness	S/N of Microhardness	Wear Volume	S/N of Wear Volume
1	347.33	50.8148	1.8152	-5.17849
2	348.23	50.8373	1.6175	-4.17689
3	381.24	51.6240	1.5803	-3.97479
4	362.63	51.1893	1.3874	-2.84403
5	385.23	51.7144	1.1864	-1.48462
6	389.13	51.8019	1.2991	-2.27285
7	414.43	52.3490	1.7939	-5.07596
8	403.60	52.1190	1.4372	-3.15034
9	428.93	52.6477	1.3288	-2.46919

3.1 ANOVA Variance Analysis

The ANOVA technique was employed to analyze the optimal data using the S/N ratio table. Before using ANOVA, the Anderson–Darling (AD) test was done to check for normality. When the p-value is greater than 0.05, it shows that the distribution is normal. The p-values from the AD test, after transforming S/N values of microhardness and wear volume, were indeed greater than 0.05, as demonstrated in Figure 5 (**a-b**). With the normal distribution of responses validated, ANOVA was performed accordingly.

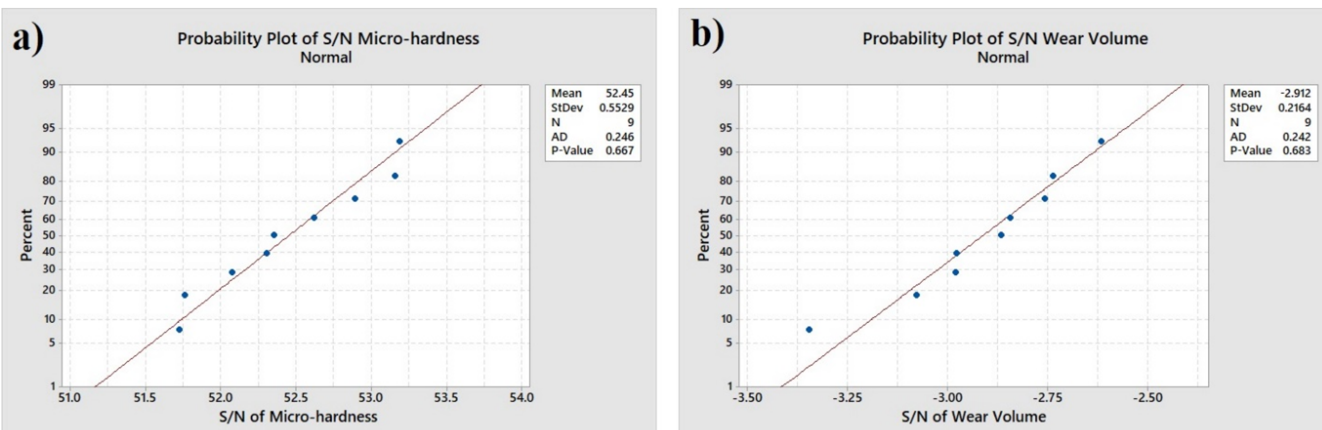

Fig 5. (a) Normality test for S/N of Hardness and, (b) Normality test for S/N of Wear volume

3.2 Influence of Control Variables on Microhardness

Table 4 displays the ANOVA results with the S/N ratio of microhardness. The p-value for laser power was 0.012, significantly lower than the 0.05 significance level, indicating that laser power had a substantial influence on microhardness. Laser power contributed 76.13% to the variance in microhardness, making it the most influential factor, followed by scanning speed of 20.49% and powder feed rate of 2.44%.

Table 4. S/N of Microhardness ANOVA analysis

Source	DF	Seq SS	Contribution	Adj SS	Adj MS	F-Value	P-Value
LP (kW)	2	4363.60	76.13%	4363.60	2181.80	81.41	0.012
SS (mm/s)	2	1174.49	20.49%	1174.49	587.25	21.91	0.044
PFR (g/m)	2	139.72	2.44%	139.72	69.86	2.61	0.277
Error	2	53.60	0.94%	53.60	26.80		
Total	8	5731.42	100.00%				

Figure 6 presents the results of averaging the S/N of microhardness for each factor at various levels. The delta value, indicating the maximum of means, ranked laser power as the most influential parameter. Figure 6 illustrates the main effect plot, showing that an increase in laser power led to a significant increase in microhardness. The desirable values were achieved at the second level of laser power, the second level of scanning speed, and the second level of the powder feed rate according to the S/N ratio effect plot. The optimal parameters were found to be 1.6 kW of laser power, 10 mm/s of scanning speed and 25 g/m of powder feed rate. The same phenomenon has been found in the research reported by Guofu Lian et al. [23].

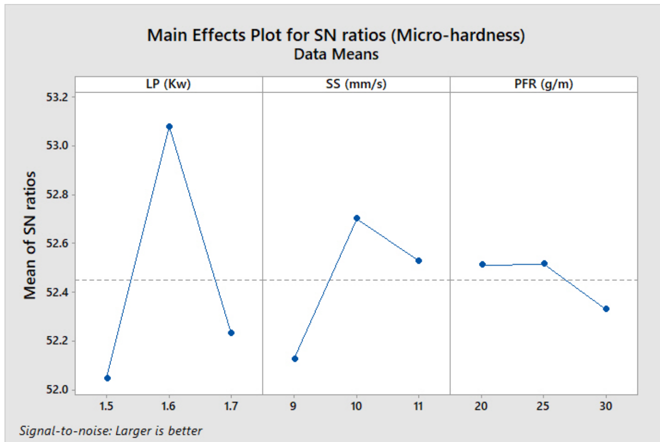

Fig 6. S/N of Microhardness with main effects plot

3.3 Influence of Control Variables on Wear Volume

In the wear volume analysis displayed in Table 5, the contribution percentages of the factors were as follows: powder feed rate - 61.99%, laser power - 18.09%, scanning speed - 16.67%, and error - 3.25%. This indicated that powder feed rate had the most significant impact on wear volume, primarily due to the use of Inconel 625 powder.

Table 5. S/N of Wear volume ANOVA analysis

Source	DF	Seq SS	Contribution	Adj SS	Adj MS	F-Value	P-Value
LP (kW)	2	0.001786	18.09%	0.001786	0.000893	5.57	0.152
SS (mm/s)	2	0.001645	16.67%	0.001645	0.000823	5.13	0.163
PFR (g/m)	2	0.006120	61.99%	0.006120	0.003060	19.07	0.050
Error	2	0.000321	3.25%	0.000321	0.000160		
Total	8	0.009872	100.00%				

Figure 7 presents the average Signal/Noise of wear volume for each factor at various levels, with powder feed rate having the highest influence. Figure 7, based on the S/N ratio response table, suggests that the third level of laser power, scanning speed and powder feed rate values are optimal for achieving high S/N ratios and lower wear volume values. An increase in powder feed rate significantly reduced wear loss, possibly due to the limitations on the plastic deformation of the AZ61 Mg alloy caused by the addition of Inconel 625. This resulted in increased hardness of the cladded structure, reducing wear loss. The similar findings are seemed to be agreed with the results reported by Guofu Lian et al. [23].

*3.3.1 **Grey Relational Analysis of Mechanical Responses***

An optimization method is presented in this study, where the grey relational analysis is combined with the Taguchi (DOE) technique. This work aimed at to simultaneously maximize microhardness and minimize wear volume. While the Taguchi orthogonal experiment design and ANOVA are effective for single-objective optimization, they fall short in multi-objective scenarios. GRA was employed to determine the best processing settings based on both microhardness and wear volume responses. The normalization technique known as GRA could be proposed as an effective strategy to optimize complex correlations among multiple performance parameters. GRA quantifies numerous performance characteristics within a Grey Relational Grade (GRG).

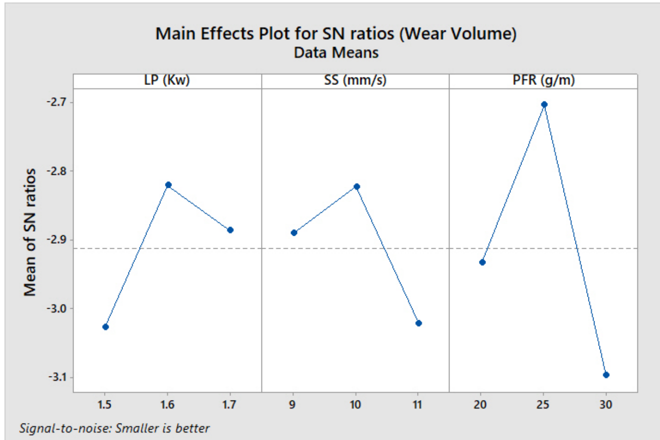

Fig 7. S/N of Wear volume with main effects plot

The steps involved in the GRA data processing are as follows:

Step – 1: S/N Ratio Normalization and Deviation

The first step in GRA involves normalizing and deviating the experimental data to fit within a range of 0-1. In this analysis, higher microhardness is equated to better cladding performance "higher-is-better", while lower wear volume also indicates better performance "lower-is-better"[24]. The normalized microhardness and wear volume values were calculated using Equations (1) and (2) respectively. The deviation sequence values are displayed in Table 6.

Larger the better option:

$$Y_i(p) = \frac{X_i(p) - minX_i(p)}{maxX_i(p) - minX_i(p)} \tag{1}$$

Smaller the better option:

$$Y_i(p) = \frac{maxX_i(p) - X_i(p)}{maxX_i(p) - minX_i(p)} \tag{2}$$

Step – 2: Calculation of the Grey Relation Coefficient (GRC):

Following the normalization of the S/N ratio, the GRC is calculated by using the Equation (3).

$$GRC_i(p) = \frac{\Delta_{min}(p) + \delta\Delta_{max}(p)}{\Delta_i(p) + \delta\Delta_{max}(p)} \tag{3}$$

Step – 3: Grey Relational Grade Calculation:

The GRG is calculated by using the Equation (4), which assigns equal weight to the responses of microhardness and wear volume.

$$GRC_i = \frac{1}{n}\sum_{p=1}^{n} GRC_i(p) \tag{4}$$

The calculated values of normalization, the GRC and the GRG for all runs are shown in Table 6. Following this, an ANOVA was conducted. Table 7 presents the analysis of the input variables and their influence on the overall grey relational grade: laser power contributed - 75.17%, powder feed rate - 16.21% and scanning speed - 7.52%. Table 6 also shows the overall GRG rank, with the fourth run being optimal, characterized by 1.6 kW of LP, 10 m/s of SP and 25 g/m of PFR. Figure 8 illustrates the rank order for GRG with mechanical responses.

Table 6. Data normalization, deviation, GRC and GRG values

Trial No.	S/N of Microhardness			S/N of Wear Volume			GRG	Rank
	Normalized	Deviation	GRC	Normalized	Deviation	GRC		
1	0.0233	0.9767	0.3386	0.5147	0.4853	0.5075	0.4230	7
2	0.3748	0.6252	0.4444	0.8113	0.1887	0.7260	0.5852	6
3	0.2256	0.7744	0.3923	0.0000	1.0000	0.3333	0.3628	9
4	0.7848	0.2152	0.6991	1.0000	0.0000	1.0000	0.8496	1
5	1.0000	0.0000	1.0000	0.6655	0.3345	0.5992	0.7996	2
6	0.9776	0.0224	0.9570	0.5122	0.4878	0.5062	0.7316	3
7	0.0000	1.0000	0.3333	0.3766	0.6234	0.4451	0.3892	8
8	0.5897	0.4103	0.5493	0.6984	0.3016	0.6238	0.5865	5
9	0.4079	0.5921	0.4578	0.8391	0.1609	0.7565	0.6072	4

Table 7. S/N of grey relational grade ANOVA analysis

Source	DF	Seq SS	Contribution	Adj SS	Adj MS	F-Value	P-Value
LP [kW]	2	0.189000	75.17%	0.189000	0.094500	68.26	0.014
SS [mm/s]	2	0.018900	7.52%	0.018900	0.009450	6.83	0.128
PFR [g/m]	2	0.040753	16.21%	0.040753	0.020377	14.72	0.064
Error	2	0.002769	1.10%	0.002769	0.001384		
Total	8	0.251422	100.00%				

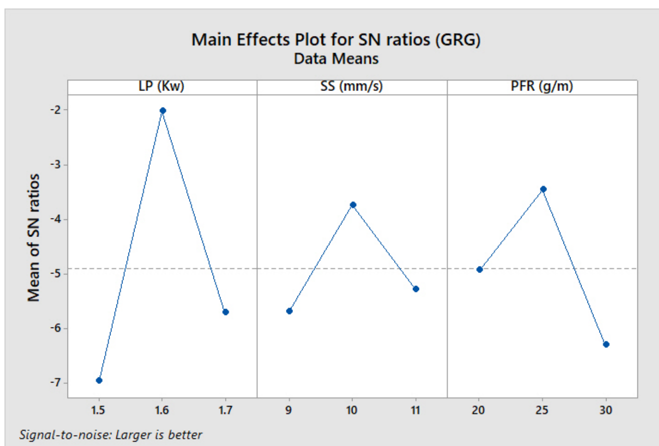

Fig 8. S/N of GRG with main effects plot

3.3.2 ***Experimental Validation***

The final step involves experimental validation and assessing the performance characteristics. Once the optimal input parameter values are obtained, this validation experiment employs the same setup with the obtained values, measuring output responses. The Table 8 showcases predicted and observed response values along with their corresponding percentage errors during the experimental validation of the developed model. The maximal error observed is 1.98%. This indicates a close relationship between predicted and observed values.

3.3.3 ***Wear Mechanism***

Wear mechanism analysis revealed that increasing the powder feed rate reduced the wear volume and improved the wear resistance by limiting plastic deformation and enhancing the protection of the AZ61 matrix. Figure 9**(a)** reveals that an increase in the powder feed rate correlates with a thicker coating and a consequent reduction in the wear rate. The presence and effect of Inconel 625 particles on the surface of the worn areas are prominently visible. These surfaces exhibited minimal plastic deformation of the Mg matrix and were characterized by grooved lines resulting from interaction with the hard counter surface.

Table 8. Experimental validation and comparison

Input Parameters / Output Responses	4^{th} run (Taguchi design)	Predicted optimal set	Experimental validation
Laser Power (kW)	1.6	1.6	1.6
Scanning Speed (mm/s)	9	10	10
Powder Feed Rate (g/m)	25	25	25
Microhardness (HV)	441.17	-	458.25
Wear volume (mm^3)	1.3515	-	1.3695
GRG	0.8496	0.9034	0.8836

As the powder feed rate of Inconel 625 particles increased, the extent of plastic drift, crater formation, and ploughing marks were noticeably diminished. This suggests that composite coatings enriched with more Inconel 625 particles provided enhanced protection to the underlying softer Mg-based alloy, resulting in less wear and the absence of deep plough grooves. Figure 9 **(b)**, however, highlights a different aspect of the wear mechanism. It shows that when the powder feed rate exceeded 25 g/min, the formation of a tribo layer was observed. This layer, while generally beneficial, had its effectiveness limited due to the aggregation of Inconel 625 particles within the matrix phase. These isolated patches of the tribo layer at the worn surface indicated that there is an optimal concentration of Inconel 625 particles for achieving the best tribological performance.

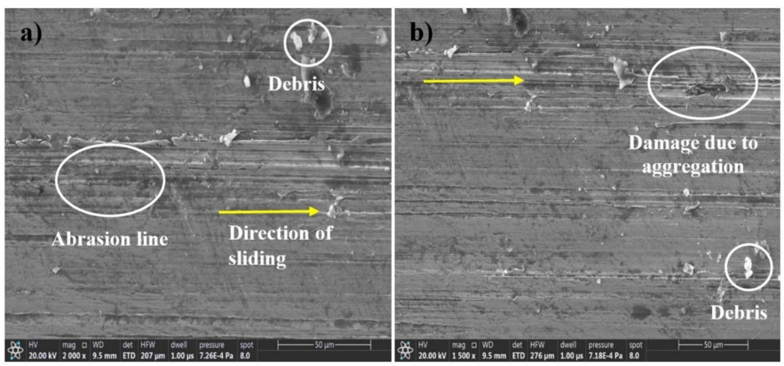

Fig 9. SEM Morphology of worn surfaces: a) Low Wear Loss, b) High Wear Loss

4 Conclusion

The research article makes use of the Taguchi orthogonal design to assess the impact of processing parameters (Laser Power, Scanning Speed and Powder Feed Rate) on the microhardness and wear volume of laser-cladded AZ61 Mg alloy. Both the signal-to-noise (S/N) ratio conversion and multi-objective grey relational analysis were utilized to optimize the maximum hardness (458.25 HV) and minimum wear volume (1.3695 mm^3). The experimental validation of the given processing parameters confirmed the effectiveness of this approach. The key conclusions drawn from this study are as follows:

1. In microhardness analysis, the primary order of processing parameters was LP, SS and PFR. Laser power implies a significant effect on the microhardness, which improved the microhardness by increasing the laser power up to 1.6 kW, after which the level of hardness lowers due to the larger melt pool formed on the substrate surface.
2. Wear volume analysis, the order of parameters was PFR, LP and SS. Powder feed rate shows a significant effect on the wear volume, reduction of wear volume by increasing the powder feed rate up to 25 g/min, after which the level of wear volume increases due to increased inclusion of particles. Insufficient melting and bonding between particles, and the formation of undesirable phases or microstructures weaken the clad layer, reduces its hardness, and ultimately decreases wear resistance.
3. In the responses of hardness and wear volume evaluation in grey relational analysis, the processing parametric orders are laser power (75.17%), powder feed rate (16.21%) and scanning speed (7.52%), with laser power and powder feed ratio being statistically significant.

4. Maximum microhardness and minimum wear volume were obtained at optimal processing parameters of 1.6 kW laser power, 10 mm/s scanning speed and 25 g/min powder feed rate.

5 Future scope of work

To investigate the mechanical, tribological and corrosion behaviors of surface-modified AZ61 reinforced with Inconel 625 by optimizing the Laser cladding process parameters of laser power (LP), scanning speed (SS), powder feed rate (PFR) and Gas flow rate (GFR) using a Taguchi (L16) experimental design for future studies.

References

1) Unnikrishnan MA, Dhas JER, Lewise KAS, Varghese JC, Ganesh M. Challenges on friction stir welding of magnesium alloys in automotives. *Materials Today: Proceedings*. 2023. Available from: https://doi.org/10.1016/j.matpr.2023.03.789.
2) Das AK. Recent trends in laser cladding and alloying on magnesium alloys: A review. *Materials Today: Proceedings*. 2022;51(Part 1):723–727. Available from: https://doi.org/10.1016/j.matpr.2021.06.217.
3) Wu T, Zhang K. Corrosion and Protection of Magnesium Alloys: Recent Advances and Future Perspectives. *Coatings*. 2023;13(9):1–32. Available from: https://doi.org/10.3390/coatings13091533.
4) Sharma P, Singh SP, Parakh SK, Tong YW. Health hazards of hexavalent chromium (Cr (VI)) and its microbial reduction. *Bioengineered*. 2022;13(3):4923–4938. Available from: https://doi.org/10.1080/21655979.2022.2037273.
5) Mouli GC, Chakradhar RPS, Srivastava M, Barshilia HC. Cold-Sprayed Cu-Zn-Al2O3 Coating on Magnesium Alloy: Enhanced Microhardness and Corrosion Behavior. *Journal of Materials Engineering and Performance*. 2023;32(14):6160–6174. Available from: https://doi.org/10.1007/s11665-022-07551-4.
6) Pranzetti A, Bellacci M, Cappuccini F, Rizzo E. Electroless Nickel Plating Applications to Enhance Corrosion Protection, Equipment Reliability and Cost Effectiveness in Centrifugal Compressors. In: ADIPEC; Paper Number: SPE-211179-MS. SPE. 2022. Available from: https://doi.org/10.2118/211179-MS.
7) Sampatirao H, Radhakrishnapillai S, Dondapati S, Parfenov E, Nagumothu R. Developments in plasma electrolytic oxidation (PEO) coatings for biodegradable magnesium alloys. *Materials Today: Proceedings*. 2021;46(Part 2):1407–1415. Available from: https://doi.org/10.1016/j.matpr.2021.02.650.
8) Riquelme A, Rodrigo P. An Introduction on the Laser Cladding Coatings on Magnesium Alloys. *Metals*. 2021;11(12):1–14. Available from: https://doi.org/10.3390/met11121993.
9) Shayanfar P, Daneshmanesh H, Janghorban K. Parameters Optimization for Laser Cladding of Inconel 625 on ASTM A592 Steel. *Journal of Materials Research and Technology*. 2020;9(4):8258–8265. Available from: https://doi.org/10.1016/j.jmrt.2020.05.094.
10) Fan P, Zhang G. Study on process optimization of WC-Co50 cermet composite coating by laser cladding. *International Journal of Refractory Metals and Hard Materials*. 2020;87:105133. Available from: https://doi.org/10.1016/j.ijrmhm.2019.105133.
11) Yi P, Zhan X, He Q, Liu Y, Xu P, Xiao P, et al. Influence of laser parameters on graphite morphology in the bonding zone and process optimization in gray cast iron laser cladding. *Optics & Laser Technology*. 2019;109:480–487. Available from: https://doi.org/10.1016/j.optlastec.2018.08.028.
12) Wu Z, Li T, Li Q, Shi B, Li X, Wang X, et al. Process optimization of laser cladding Ni60A alloy coating in remanufacturing. *Optics & Laser Technology*. 2019;120:105718. Available from: https://doi.org/10.1016/j.optlastec.2019.105718.
13) Sundaraselvan S, Senthilkumar N, Tamizharasan T, Sait AN. Surface modification of AZ61 Magnesium Alloy with Nano TiO2/Al2O3 using Laser Cladding Technique. *Materials Today: Proceedings*. 2020;21(Part 1):717–721. Available from: https://doi.org/10.1016/j.matpr.2019.06.745.
14) Asghar O, Li-Yan L, Yasir M, Chang-Jiu L, Cheng-Xin L. Enhanced Tribological Properties of LA43M Magnesium Alloy by Ni60 Coating via Ultra-High-Speed Laser Cladding. *Coatings*. 2020;10(7):1–14. Available from: https://doi.org/10.3390/coatings10070638.
15) Bu R, Jin A, Sun QA, Zan W, He R. Study on laser cladding and properties of AZ63-Er alloy for automobile engine. *Journal of Materials Research and Technology*. 2020;9(3):5154–5160. Available from: https://doi.org/10.1016/j.jmrt.2020.03.032.
16) Riquelme A, Rodrigo P, Escalera-Rodriguez MD, Rams J. Evaluation of the Wear Resistance and Corrosion Behavior of Laser Cladding Al/SiC Metal Matrix Composite Coatings on ZE41 Magnesium Alloy. *Coatings*. 2021;11(6):1–19. Available from: https://doi.org/10.3390/coatings11060639.
17) Liu H, Tan CKI, Wei Y, Lim SH, Lee CJJ. Laser-cladding and interface evolutions of inconel 625 alloy on low alloy steel substrate upon heat and chemical treatments. *Surface and Coatings Technology*. 2020;404:126607. Available from: https://doi.org/10.1016/j.surfcoat.2020.126607.
18) Kotarska A, Poloczek T, Janicki D. Characterization of the Structure, Mechanical Properties and Erosive Resistance of the Laser Cladded Inconel 625-Based Coatings Reinforced by TiC Particles. *Materials*. 2021;14(9):1–16. Available from: https://doi.org/10.3390/ma14092225.
19) Yang B, Lai Y, Yue X, Wang D, Zhao Y. Parametric Optimization of Laser Additive Manufacturing of Inconel 625 Using Taguchi Method and Grey Relational Analysis. *Scanning*. 2020;2020:1–10. Available from: https://doi.org/10.1155/2020/9176509.
20) Bloemer PRA, Pacheco JT, Cunha A, Veiga MT, Filho OCDM, Meura VH, et al. Laser Cladding of Inconel 625 on AISI 316L: Microstructural and Mechanical Evaluation of Parameters Estimated by Empirical-Statistical Model. *Journal of Materials Engineering and Performance*. 2022;31(1):211–220. Available from: https://doi.org/10.1007/s11665-021-06147-8.
21) Singh AK, Sadhu A, Das AK, Pratihar DK, Choudhury AR. An approach towards energy and material efficient additive manufacturing: Multi-objective optimization of stellite-6 deposition on SS304. *Optics & Laser Technology*. 2022;148:107799. Available from: https://doi.org/10.1016/j.optlastec.2021.107799.
22) Samuel SC, Arivarasu M, Prabhu TR. High temperature dry sliding wear behaviour of laser powder bed fused Inconel 718. *Additive Manufacturing*. 2020;34:101279. Available from: https://doi.org/10.1016/j.addma.2020.101279.
23) Lian G, Xiao S, Zhang Y, Jiang J, Zhan Y. Multi-objective optimization of coating properties and cladding efficiency in 316L/WC composite laser cladding based on grey relational analysis. *The International Journal of Advanced Manufacturing Technology*. 2021;112(5-6):1449–1459. Available from: https://doi.org/10.1007/s00170-020-06486-1.
24) Mugilan T, Sridhar N, Sathishkumar GB. Multi response hybrid optimization of sustainable high-speed end milling on 89.7Ti-6Al-4V. *Materials Today: Proceedings*. 2022;65(Part 8):3170–3176. Available from: https://doi.org/10.1016/j.matpr.2022.05.362.